Supporting Information

Dissociative Chemisorption of O_2 on Al(111): Dynamics on A Correlated Wavefunction Based Potential Energy Surface

Rongrong Yin,[1] Yaolong Zhang,[1] Florian Libisch,[2] Emily A. Carter,[3] Hua Guo,[4] Bin Jiang[1,*]

[1]*Hefei National Laboratory for Physical Science at the Microscale, Department of Chemical Physics, University of Science and Technology of China, Hefei, Anhui 230026, China*

[2]*Institute for Theoretical Physics, Vienna University of Technology, 1040 Vienna, Austria*

[3]*School of Engineering and Applied Science, Princeton University, Princeton, New Jersey 08544-5263, United States*

[4]*Department of Chemistry and Chemical Biology, University of New Mexico, Albuquerque, New Mexico 87131, United States*

*: corresponding author, email: bjiangch@ustc.edu.cn

I. Computational Details

A. Embedded Correlated Wavefunction Theory

Embedded Correlated Wavefunction (ECW) theory combines the high accuracy of correlated wavefunction (CW) calculations on clusters with a periodic density functional theory (DFT) description of the extended metal surface.[1] Specifically, we put the O_2 molecule above a small cluster of 10 to 14 atoms embedded in an Al(111) slab with a periodic 5×5 supercell and four metal layers,[2, 3] and first treat the entire system with DFT (E_{tot}^{DFT}). An embedding potential (V_{emb}) mediates the interaction between the cluster and its environment following density-functional embedding theory.[4] The energy of the cluster itself is computed by second-order multi-reference many-body perturbation theory[5] as well as DFT, both in the presence of V_{emb}, yielding $E_{cluster}^{CW,emb}$ and $E_{cluster}^{DFT,emb}$, respectively. The ECW total energy thus is expressed as,

$$E_{tot}^{CW,emb} = E_{tot}^{DFT} + (E_{cluster}^{CW,emb} - E_{cluster}^{DFT,emb}) . \quad \text{(S1)}$$

More details of the ECW theory and convergence tests can be found in Refs 1, 2 and 3.

B. Potential Energy Surface

Fig. S1 depicts the structure of the Al(111) facet and the dynamical coordinates describing the O_2 dissociative chemisorption. To construct the potential energy surface (PES), we collect over 700 single points over three high-symmetry sites from Refs. 2 and 3. These data include four two-dimensional (2D) cuts as a function of the Al-O ($d_{\text{Al-O}}$) and O-O distances (r) with the O_2 molecule lying either parallel or perpendicular above the fcc site, as well as 2D cuts at the bridge and top sites with parallel O_2 orientation as a function of the height of the molecular center of mass (z) and r. Also included are the data representing different molecular orientations

as a function of the polar angle (θ) and azimuthal angle (φ), with r=1.3 Å and $d_{\text{Al-O}}$ varying from 1.5 to 2.5 Å.

Because ECW calculations are much more expensive than conventional DFT, the number of points is limited. As a result, two widely applied approaches, *i.e.*, neural networks (NNs) [6-9] and the corrugation reducing procedure (CRP)[10, 11] for generating global PESs are not amenable, because they require at least a few thousand points to achieve a reasonable fit. Unphysical holes may appear in regions where the ab initio data are sparse. Instead, we chose here the flexible periodic London-Eyring-Polanyi-Sato (FPLEPS) function,[12, 13] which is analytical and requires about one order of magnitude fewer ab initio points than NNs and CRP. The physically inspired LEPS function was adapted to deal with simple diatom-surface interactions by McCreery and Wolken in 1970s when ab initio data were rather scarce.[14] Unfortunately, this over-simplified form lacks the flexibility for accurately describing the more complicated topography of realistic surfaces, in particular the dependence on the exact adsorption site. Martin-Gondre *et al*. recently extended the LEPS form with site-dependent Sato parameters and Gaussian functions to better represent the barrier corrugation and entrance channel.[12, 13] The FPLEPS approach has been validated by correctly reproducing important features of the CRP PESs for N_2/W(100), N_2/W(110), H_2/W(100) and H_2/W(110) systems,[12, 13] as well as dynamics in both dissociative chemisorption and Eley-Rideal reactions.[15]

For describing the interaction of the surface with two atoms, here Al(111) with O_A and O_B, the original LEPS potential[16] $V(r_{O_A}, r_{O_B}, r_{O_A\text{-}O_B})$ can be written as:

$$V(r_{O_A}, r_{O_B}, r_{O_A\text{-}O_B}) = U_{O_AAl}(r_{O_A}) + U_{O_BAl}(r_{O_B}) + U_{O_2}(r_{O_A\text{-}O_B}) - \sqrt{Q_{O_2}{}^2(r_{O_A\text{-}O_B}) + \left(Q_{O_AAl}(r_{O_A}) + Q_{O_BAl}(r_{O_B})\right)^2 - Q_{O_2}(r_{O_A\text{-}O_B})\left(Q_{O_AAl}(r_{O_A}) + Q_{O_BAl}(r_{O_B})\right)} \quad \text{(S2)}$$

where the U_i (Q_i) represent the Coulomb (exchange) integrals for two-body interactions ($i = \mathrm{O_A Al},\ \mathrm{O_B Al},\ \mathrm{O_2}$):

$$U_i = \frac{D_i}{4(1+\Delta_i)}\left[(3+\Delta_i)\exp(-2\alpha_i(r_i - r_i^{eq})) - (2+6\Delta_i)\exp(-\alpha_i(r_i - r_i^{eq}))\right], \quad \text{(S3)}$$

$$Q_i = \frac{D_i}{4(1+\Delta_i)}\left[(1+3\Delta_i)\exp(-2\alpha_i(r_i - r_i^{eq})) - (6+2\Delta_i)\exp(-\alpha_i(r_i - r_i^{eq}))\right] \quad \text{(S4)}$$

.

D_i, α_i, r_i^{eq} are the Morse parameters, namely the well depth, the range of the attractive part of the potential and the equilibrium distance between two bodies O_2, O_AAl, or O_BAl, where Al here denotes the first aluminum layer and OAl is the height of each O atom above the surface. The three Sato parameters (Δ_i) essentially determine the barrier heights and locations along the reaction pathways. The periodic dependence is incorporated in the Morse potential by expressing the Morse parameters by a Fourier expansion in terms of the lattice vectors *u* and *v* (labelled in Fig. S1). For an fcc(111) facet within the approximation that the fcc and hcp sites are identical, for example, the Fourier expansion is given as,[17]

$$\begin{aligned} p_j(u,v) = P_0 &+ P_1\left[\cos\frac{2\pi u}{L} + \cos\frac{2\pi v}{L} + \cos\frac{2\pi(u+v)}{L}\right] \\ &+ P_2\left[\cos\frac{4\pi u}{L} + \cos\frac{4\pi v}{L} + \cos\frac{4\pi(u+v)}{L}\right] \end{aligned}, \quad \text{(S5)}$$

where L is the nearest-neighbor distance between two surface atoms, and the expansion coefficients P_0, P_1, P_2 are obtained by solving a set of linear equations once we find the Morse parameters for three high symmetry sites (top, bridge, and hollow). Following Martin-Gondre *et al.*,[12, 13] we include a dependence on the bond length r_i in α_i to better describe the one-

dimensional O-O and O-Al interactions, *i.e.*, $\alpha_i(r_i) = \alpha_i^0 + \alpha_i^1 r_i$ where the two additional parameters α_i^0 and α_i^1 are also optimized.

The choice of the Sato parameters is of essential importance in representing the global PES. In the FPLEPS function, the periodicity is also incorporated into the Sato parameters, thus offering more flexibility: the site-dependent Sato parameters at the top, bridge, and hollow sites differ and the Fourier expansion in Eq. (S5) again yields the correct periodicity. In addition, there is a shallow physisorption well in the entrance channel in this system, which is not intrinsically described in the LEPS framework. We therefore add a negative Gaussian function with respect to the height of the molecule in the final form of the PES,[12, 13]

$$G(z) = A\exp\left[-\frac{(z - z_0)^2}{\sigma^2}\right], \tag{S6}$$

where A, σ, and z_0 are the amplitude, width, and center of the Gaussian, which represent the well depth, shape and location, respectively. Note that the Gaussian function is also site-dependent just like the adsorption well. These parameters shaping the FPLEPS function are all optimized using the non-linear Levenberg-Marquardt algorithm[18] which minimizes the discrepancies between the energy values predicted by the FPLEPS function and the original CW data. The optimized parameters are reported in Table S1.

C. Dynamics

To validate the FPLEPS PES, extensive quasi-classical trajectory (QCT) calculations have been performed to simulate the dissociative chemisorption dynamics of O_2 on Al(111). The trajectories were initiated at 6.0 Å above the surface with the molecular center randomly chosen to cover the 1×1 unit cell. The diatomic molecule is treated as a rotating oscillator, whose

internal energy was calculated semi-classically as a function of vibrational and rotational quantum numbers v and j.[19] Different initial states and incidence conditions were chosen to simulate different experiments. To compare with the experimental results of Österlund *et al.*[20] obtained with a conventional molecular beam, we use as the initial condition a randomly oriented, ground ro-vibrational state of O_2 impinging along the surface normal with an incident energy ranging from 0.05 eV to 1.0 eV. Simulating the measurements of Kurahashi and Yamauchi[21] who used a spin-rotational-state-selected molecular beam, we select the specific rotational state (v=0, j=1, m_j=1) and vary the incident angle from $\alpha=0^\circ$ (surface normal) to $\alpha=40^\circ$ with the azimuthal angle fixed in the $[1\bar{1}0]$ plane. According to the definition in Ref. 21, the helicopter and cartwheel geometries correspond to the O_2 (j=1, m_j=1) rotating about the surface normal and about the axis in the $\left[11\bar{2}\right]$ plane perpendicular to the surface normal, respectively. As a consequence, the O_2 molecule lies parallel to the surface in the helicopter orientation, while both parallel and perpendicular orientations coexist in the cartwheel geometry. The sticking probabilities for the helicopter geometry [$S_0(H)$] and random orientation [$S_0(R)$] are readily calculated from QCT, while those for the cartwheel [$S_0(C)$] and perpendicular [$S_0(P)$] geometries can be deduced as follows,[21]

$$S_0(R)=\frac{1}{3}S_0(H)+\frac{2}{3}S_0(C) \tag{S7}$$

$$S_0(P)=2S_0(C)-S_0(H) \tag{S8}$$

In all calculations, a trajectory is terminated when the molecular bond length increases to 2.5 Å (dissociation), or when the molecule-surface separation increases beyond 6.0 Å (reflection). Note that the influence of substrate motion is neglected here within the frozen surface approximation.

This is partially justified by a very weak dependence of the sticking probability on the surface temperature observed in experiment.[20] A small number of ab initio molecular dynamics trajectories also revealed that surface movements only become prominent when the O_2 molecule is quite close to the surface after dissociation.[22] In addition, low energy electron-hole pair excitations are also neglected here, which only play a minor role in the activated dissociation of molecules on metal surfaces with significant barriers.[23, 24]

II. Additional results

We further investigate the anisotropy of the PES at the hollow site in both the entrance and product channels (see Figure S2). Following Cheng et al.,[3] several PES 2D cuts are plotted as a function of θ and φ with different $d_{\text{Al-O}}$ values and r=1.3 Å, which represent the entrance channel (see Figure S2a-d). Specifically, when the molecule is far away from the surface (Figure S2a), *e.g.*, $d_{\text{Al-O}}$=2.25 Å, there is only one local minimum, *i.e.*, the //3 orientation. As the O_2 moves closer to the Al(111) surface (Figure S2b-d), the //2 configuration becomes increasingly attractive, ultimately forming a new local well attributed to the increasing overlap between the π^* orbital of O_2 and the metal orbitals when approaching parallel to the surface.[3] O_2 therefore tends to rotate from the //3 to the //2 orientation as the molecule approaches the surface preferentially from the //3 pathway. By contrast, O_2 approaching the surface with the perpendicular orientation ($\perp$) is less favorable, due to the higher barrier height in this pathway.[3]

In the product channel, the PES cuts are plotted as a function of θ and r at the fcc site for //3 geometry (φ=-30°) (see Figures S2e-f). Interestingly, the adsorbate tends to rotate from the parallel to a tilted geometry after overcoming the lowest barrier, as evidenced by the local minima θ=~70° in Figures S2e-f with the extended O-O distance. As suggested by some of the

current authors,[3] this offers the possibility of an abstraction channel, which yields a single adsorbed O atom and an oxygen atom emitted to the gas phase.[25] Overall, our FPLEPS PES 2D cuts demonstrate a strong dependence of the barrier on the angular coordinates, which are in general accord with the earlier analyses based on the original ECW data.[3] The preference of certain parallel orientations over the perpendicular ones could serve as the origin of the experimentally observed steric effect, as discussed in the main text.

References

(1) Libisch, F.; Huang, C.; Carter, E. A., Embedded correlated wavefunction schemes: Theory and applications, *Acc. Chem. Res.* **2014,** *47*, 2768-2775.

(2) Libisch, F.; Huang, C.; Liao, P.; Pavone, M.; Carter, E. A., Origin of the energy barrier to chemical reactions of O_2 on Al(111): Evidence for charge transfer, not spin selection, *Phys. Rev. Lett.* **2012,** *109*, 198303.

(3) Cheng, J.; Libisch, F.; Carter, E. A., Dissociative adsorption of O_2 on Al(111): The role of orientational degrees of freedom, *J. Phys. Chem. Lett.* **2015,** *6*, 1661-1665.

(4) Huang, C.; Pavone, M.; Carter, E. A., Quantum mechanical embedding theory based on a unique embedding potential, *J. Chem. Phys.* **2011,** *134*, 154110.

(5) Andersson, K.; Malmqvist, P. Å.; Roos, B. O., Second‐order perturbation theory with a complete active space self‐consistent field reference function, *J. Chem. Phys.* **1992,** *96*, 1218-1226.

(6) Lorenz, S.; Scheffler, M.; Gross, A., Descriptions of surface chemical reactions using a neural network representation of the potential-energy surface, *Phys. Rev. B* **2006,** *73*, 115431.

(7) Jiang, B.; Guo, H., Permutation invariant polynomial neural network approach to fitting potential energy surfaces. III. Molecule-surface interactions, *J. Chem. Phys.* **2014,** *141*, 034109.

(8) Jiang, B.; Hu, X.; Lin, S.; Xie, D.; Guo, H., Six-dimensional quantum dynamics of dissociative chemisorption of H_2 on Co(0001) on an accurate global potential energy surface, *Phys. Chem. Chem. Phys.* **2015,** *17*, 23346-23355.

(9) Liu, T. H.; Fu, B. N.; Zhang, D. H., Six-dimensional potential energy surface of the dissociative chemisorption of HCl on Au(111) using neural networks, *Sci. China: Chem.* **2014,** *57*, 147-155.

(10) Busnengo, H. F.; Salin, A.; Dong, W., Representation of the 6D potential energy surface for a diatomic molecule near a solid surface, *J. Chem. Phys.* **2000,** *112*, 7641-7651.

(11) Díaz, C.; Pijper, E.; Olsen, R. A.; Busnengo, H. F.; Auerbach, D. J.; Kroes, G.-J., Chemically accurate simulation of a prototypical surface reaction: H_2 dissociation on Cu(111), *Science* **2009,** *326*, 832-834.

(12) Martin-Gondre, L.; Crespos, C.; Larregaray, P.; Rayez, J. C.; van Ootegem, B.; Conte, D., Is the LEPS potential accurate enough to investigate the dissociation of diatomic molecules on surfaces?, *Chem. Phys. Lett.* **2009,** *471*, 136-142.

(13) Martin-Gondre, L.; Crespos, C.; Larregaray, P.; Rayez, J. C.; Conte, D.; van Ootegem, B., Detailed description of the flexible periodic London-Eyring-Polanyi-Sato potential energy function, *Chem. Phys.* **2010,** *367*, 136-147.

(14) McCreery, J. H.; Wolken, G., Model Potential for Chemisorption - H2+W(001), *J. Chem. Phys.* **1975,** *63*, 2340-2349.

(15) Pétuya, R.; Larrégaray, P.; Crespos, C.; Busnengo, H. F.; Martínez, A. E., Dynamics of H_2 Eley-Rideal abstraction from W(110): Sensitivity to the representation of the molecule-surface potential, *J. Chem. Phys.* **2014,** *141*, 024701.

(16) Kuntz, P. J.; Nemeth, E. M.; Polanyi, J. C.; Rosner, S. D.; Young, C. E., Energy distribution among products of exothermic reactions. II. Repulsive, mixed, and attractive energy release, *J. Chem. Phys.* **1966,** *44*, 1168-1184.

(17) Dai, J.; Zhang, J. Z. H., Quantum adsorption dynamics of a diatomic molecule on surface: Four-dimensional fixed-site model for H_2 on Cu(111), *J. Chem. Phys.* **1995,** *102*, 6280-6289.

(18) Zhang, Y.-l.; Zhou, X.-y.; Jiang, B., Accelerating the Construction of Neural Network Potential Energy Surfaces: A Fast Hybrid Training Algorithm, *Chin. J. Chem. Phys.* **2018,** *30*, 727-734.

(19) Hase, W. L., Classical Trajectory Simulations: Initial Conditions. In *Encyclopedia of Computational Chemistry*, Alinger, N. L., Ed. Wiley: New York, 1998; Vol. 1, pp 399-402.

(20) Österlund, L.; Zoric-acute, I.; Kasemo, B., Dissociative sticking of O_2 on Al(111), *Phys. Rev. B* **1997,** *55*, 15452-15455.

(21) Kurahashi, M.; Yamauchi, Y., Steric effect in O_2 sticking on Al(111): Preference for parallel geometry, *Phys. Rev. Lett.* **2013,** *110*, 246102.
(22) Behler, J.; Delley, B.; Lorenz, S.; Reuter, K.; Scheffler, M., Dissociation of O_2 at Al(111): The role of spin selection rules, *Phys. Rev. Lett.* **2005,** *94*, 036104.
(23) Juaristi, J. I.; Alducin, M.; Muiño, R. D.; Busnengo, H. F.; Salin, A., Role of electron-hole pair excitations in the dissociative adsorption of diatomic molecules on metal surfaces, *Phys. Rev. Lett.* **2008,** *100*, 116102.
(24) Jiang, B.; Alducin, M.; Guo, H., Electron–hole pair effects in polyatomic dissociative chemisorption: Water on Ni(111), *J. Phys. Chem. Lett.* **2016,** *7*, 327-331.
(25) Komrowski, A. J.; Sexton, J. Z.; Kummel, A. C.; Binetti, M.; Weiße, O.; Hasselbrink, E., Oxygen abstraction from dioxygen on the Al(111) surface, *Phys. Rev. Lett.* **2001,** *87*, 246103.

Table S1. Parameters of the FPLEPS PES.

Parameters	O-O	O/O_2-Al(111)		
		Top	Bridge	Hollow
D_i (eV)	4.727	1.0484	6.416	5.115
α_i^0 (Å^{-1})	2.15	3.196	0.925	0.484
α_i^1 (Å^{-2})	0.352	-0.310	0.0372	0.373
r_i^{eq} (Å^{-1})	1.267	1.687	0.853	1.082
$\Delta_{O\text{-}O}$		0.667	-0.316	0.0315
$\Delta_{O\text{-}Al}$		-0.001	-0.074	-0.071
A (eV)		-0.066	-0.130	-0.149
z_0 (Å)		3.4	3.5	3.5
σ (Å)		0.85	0.85	0.85

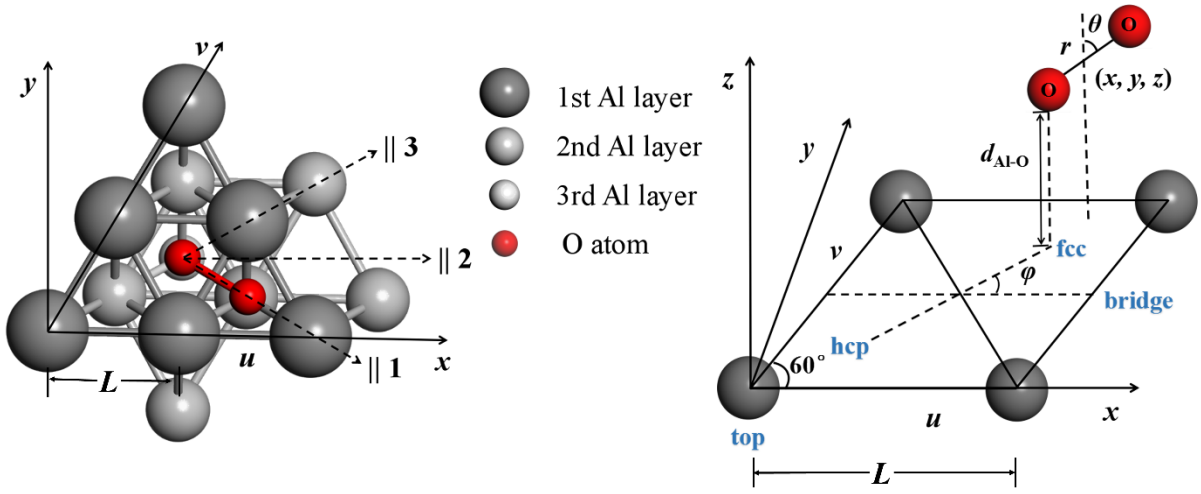

Figure S1. Definition of three different orientations above the fcc site on the top view of Al(111) (left panel) and the coordinate system for describing the O_2 dissociation on Al(111) (right panel).

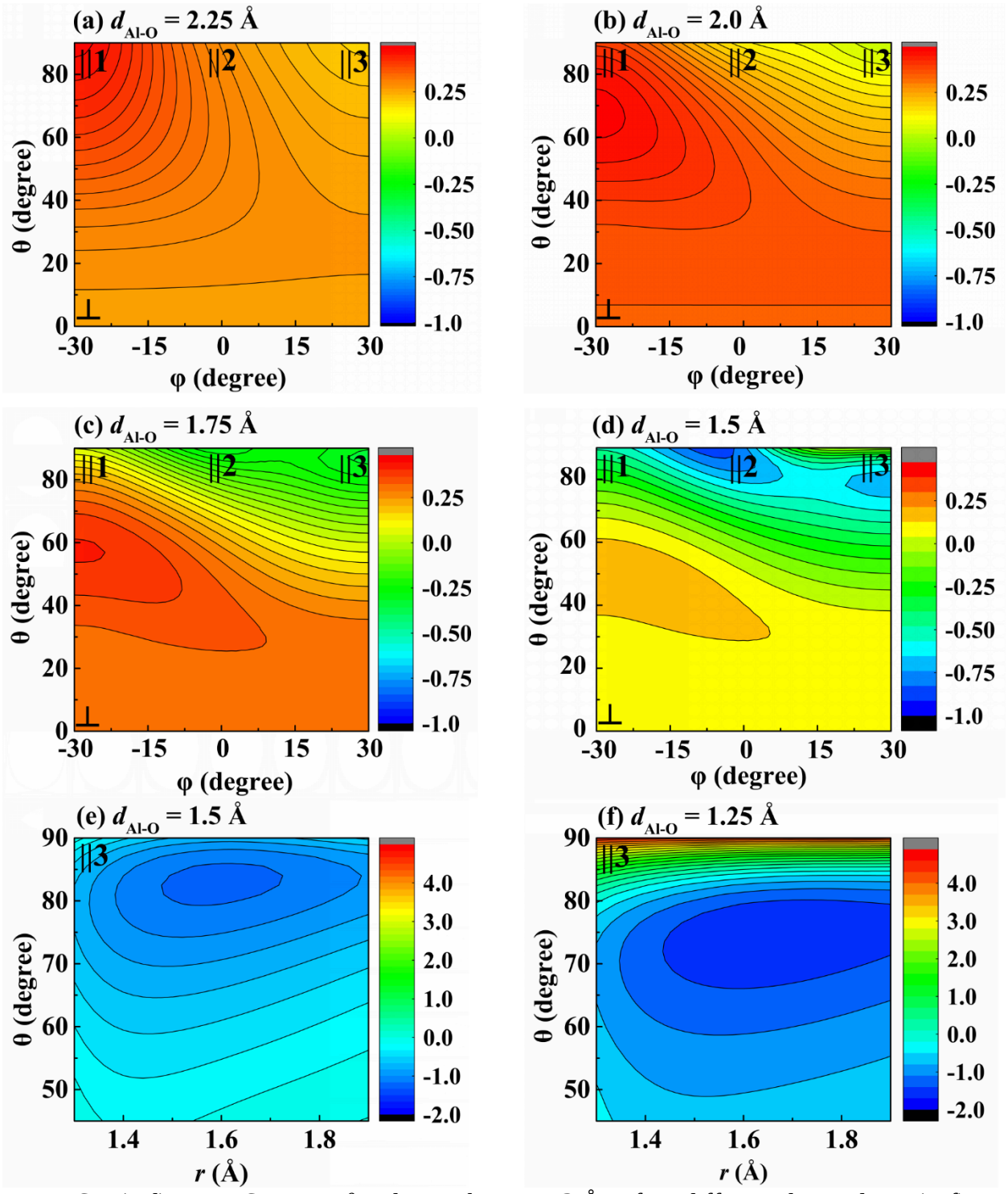

Figure S2. (a-d) 2D PES cuts in θ and φ, with r_{O-O}=1.3 Å at four different d_{Al-O} values; (e, f) 2D PES cuts in θ and r, with φ=30º (// 3 orientation) at two d_{Al-O} values. Energies are in eV.